Response to the Reviews on "Bias Correction of Gauge-based Gridded Product to Improve Extreme Precipitation Analysis in the Yarlung Tsangpo-Brahmaputra River Basin"

(nhess-2019-327)

Responses to Editor

The paper has been well improved, and this is acknowledged by the referees. However, I agree with reviewer 1 about the insufficient proof of the efficiency of the correction with the chosen protocol. One possible way of improvement could be, for the left out station, to compare the indices obtained from the series reconstructed by interpolation before and after correction, so that the role of the correction can be more clearly separated from that of the spatial interpolation. This may not be a major revision, except if no real improvement is found after correction.

Response: Thank you for the comments concerning our manuscript entitled "Bias Correction of Gauge-based Gridded Product to Improve Extreme Precipitation Analysis in the Yarlung Tsangpo-Brahmaputra River Basin" (ID: nhess-2019-327). Those comments are all valuable and very helpful. To improve the paper, we have used a cross-validation in time instead of a spatial leave one-out cross validation to evaluate the performance of different bias correction methods. In addition, we have made some other corrections.

Responses to Reviewer 1

The authors have implemented the simpler of the two suggested cross-validation options. The results from the new analysis support the authors' earlier claims. I now find that this work is fit for publication. I would, however, suggest to the authors to have their manuscript professionally edited. Slight changes in syntax will improve legibility.

Response: Thank you again for your valuable and helpful comments concerning our manuscript. We have further made some changes in syntax to improve the paper.

Responses to Reviewer 2

1. Summary

The paper by Luo X. and al proposes to compare the performance of four bias correction methods (Linear Scaling, Local Intensity Scaling, Power transformation and Quantile Mapping) of daily

precipitations during 1951-2015 over Yarlung Tsangpo-Brahmaputra River Bassin (YBRB). The data to correct comes from the gridded APHRODITE dataset, and the reference dataset are sparse observations from meteorological stations. The performance of bias correction methods is evaluated with a spatial leave one-out cross validation method: one station is removed, and an IDW interpolation between others bias corrected grid point is applied to build them.

Response: Thank you again for your valuable and helpful comments concerning our manuscript. We have carefully studied comments and made corrections, and the performance of bias correction methods were evaluated by a cross-validation in time instead of a spatial leave one-out cross validation.

2. General comments

Having already participated in the first review round, I am glad to see that my comments have been taken into account. The main addition is the leave one-out cross validation. Contrary to the usual practice, instead of a cross-validation in time (the dataset is split into two time periods, which makes it possible to check the stationarity of the probability distribution in the context of this paper), the authors propose a leave one-out cross validation by removing alternatively one station from observational data.

I'm not convinced this approach can validate the quality of bias correction. Eventually, this method can be applied if the bias correction method is multivariate (dependence structure between grid points is also corrected, with methods as MBCn, R2D2 or dOTC, see Cannon, Vrac and Robin). In this context, it is not the bias correction method that is tested, but the interpolation method.

I'm sorry, but I can not understand why the authors can not split the dataset into two time periods even if it means removing stations when no data is available for the sub time period. Furthermore, cutting does not require the sub-periods to be continuous. The heart of this paper is the improvement due to a bias correction, and the prerequisite is to verify that the method reproduces well the distribution of the observations. The only element in this sense is the figure 6, which shows a better coherence with the topography.

I can not recommend publication without a clear proof of improvement compared to observations, and it is not the case (all the figures show a modification compared to APHRODITE, but do not show if it is closed to observations, or more realistic).

Response: To better compare the extreme precipitation indices calculated from corrected APHRODITE estimates with those from observations, we have applied a cross-validation in time instead of a spatial leave one-out cross validation. At each rainfall station, the observations were divided into two groups. Two third of the rainfall records were applied to calculate the parameters of bias correction, and then APHRODITE estimates were corrected. Making use of the remaining rainfall observations, the mean error (*ME*) of the extreme precipitation indices for corrected APHRODITE estimates were calculated to evaluate the performance of different bias correction methods. Fig. 5 was redrawn to show the *ME* of extreme precipitation indices for validation.

The results showed that bias correction greatly improved the performance of extreme precipitation analysis, and local intensity scaling (LOCI) and quantile−quantile mapping (QM) performed better than linear scaling (LS) and power transformation (PT).

3. Specific comments

(1) Lines 188-189

The sentence "according to the location and observation time." is not really clear. It is my understanding that the authors correct only the grid points of APHRODITE that contain a time series of observations (and an interpolation is used for others), but I am note sure. Please clarify.

Response: We have modified the sentence as "This study corrected the grids of the APHRODITE estimates that contained time series of observations".

(2) Lines 207-209

The sentence "To obtain extreme precipitation indices in other grids with no rainfall station distributed, spatial interpolation was performed using inverse distance weighted (IDW) interpolation" is slightly confusing. You perform the interpolation between the bias corrected dataset or between the extreme precipitation indices computed from the bias corrected dataset?

Response: We have modified the sentence as "To obtain extreme precipitation indices in other grids, inverse distance weighted (IDW) interpolation for extreme precipitation indices were performed".

4. Technical comments

Figure 4

In the x-label: correction instead of "coeeection".

Response: We have replaced "coeeection" with "correction" in the x-label in Figure 4. Thanks for all of your suggestions.

Title

Bias correction of gauge-based gridded product to improve extreme precipitation analysis in the

Yarlung Tsangpo-Brahmaputra River Basin

Author names and affiliations

Xian Luo[1,2], Xuemei Fan[1], Yungang Li[1,2], and Xuan Ji[1,2]

[1]Institute of International Rivers and Eco-security, Yunnan University, Kunming, China

[2]Yunnan Key Laboratory of International Rivers and Transboundary Eco-security, Kunming, China

Address

Institute of International Rivers and Eco-security, Yunnan University,

South Section, East Outer Ring Road, Chenggong District, Kunming, China

Email

Xian Luo: luoxian@ynu.edu.cn

Xuemei Fan: fanxuemei7@163.com

Yungang Li: ygli@ynu.edu.cn

Xuan Ji: jixuan@ynu.edu.cn

Contact Author: Xian Luo (luoxian@ynu.edu.cn)

Second Contact Author: Yungang Li (ygli@ynu.edu.cn)

Abstract. Critical gaps in the amount, quality, consistency, availability, and spatial distribution of rainfall data limit extreme precipitation analysis, and the application of gridded precipitation data are challenging because of their considerable biases. This study corrected Asian Precipitation Highly Resolved Observational Data Integration Towards Evaluation of Water Resources (APHRODITE) estimates in the Yarlung Tsangpo-Brahmaputra River Basin (YBRB) using two linear and two nonlinear methods, and their influence on extreme precipitation indices were assessed by cross-validation. Bias correction greatly improved the performance of extreme precipitation analysis. The ability of four methods to correct wet-day frequency and coefficient of variation were substantially different, leading to considerable differences in extreme precipitation indices. Local intensity scaling (LOCI) and quantile−quantile mapping (QM) performed better than linear scaling (LS) and power transformation (PT). This study would provide reference for using gridded precipitation data in extreme precipitation analysis and selecting bias-corrected method for rainfall products in data-sparse regions.

1   Introduction

Extreme precipitation often leads to floods, debris flows, and other secondary disasters (Wang et al., 2017), and changes in the frequency and intensity of extreme precipitation profoundly influence both natural environment and human society profoundly (Easterling et al., 2000; Yucel and Onen, 2014). Rainfall observations provide a primary foundation for comprehending their long-term variability and change in extreme precipitation (Alexander, 2016). Accurate rainfall data are necessary for flood protection and water resource management. However, due to scarce spatial coverage of rainfall stations, short-length rainfall records, and high proportions of missing data,

observations currently available in some remote basins are clearly inadequate to capture their precipitation characteristics. In addition, observed rainfall data are usually difficult to collect in international river basins because many countries may not share or freely distribute data (Lakshmi et al., 2018).

The Yarlung Tsangpo-Brahmaputra River is the fourth largest river in the world in terms of flow (Kamal-Heikman et al., 2007), which is influenced profoundly by complex atmospheric dynamics and regional climate processes (Immerzeel et al., 2010; Pervez and Henebry, 2015). Because its agriculture and economy rely heavily on monsoon precipitation, the basin is particularly vulnerable to changing climate (Singh et al., 2016; Liu et al., 2018; Janes et al., 2019; Xu et al., 2019; Zhang et al., 2019). During the four summer monsoon months of June, July, August, and September (JJAS), extreme precipitation with large uncertainties lead to numerous floods (Kamal-Heikman et al., 2007; Dimri et al., 2016; Malik et al., 2016). However, the understanding on extreme precipitation in the Yarlung Tsangpo-Brahmaputra River Basin (YBRB) have a number of gaps because of its complex topographic interactions with atmospheric flows, lack of observations, and data sharing issues, which hinder effective flood management (Ray et al., 2015; Prakash et al., 2019).

Currently, different gridded rainfall products provide effective information over regional to global scales, which could be broadly classified into four categories: (1) gauge-based data sets that build on observations from rainfall stations; (2) products from numerical weather predictions or atmospheric models; (3) satellite-only products; and (4) combined satellite-gauge products. The performance of these products vary from region to region (Duan et al., 2016). Given the heterogeneity of orography and climate in the YBRB, observing and modeling its precipitation are very challenging (Khandu et al., 2017). In addition, satellite products are less reliable because high

convective rainfall generally takes place in the southern foothills of the Himalayas (Prakash et al.,

2015). Compared with some other gauge-based products, Asian Precipitation Highly Resolved

Observational Data Integration Towards Evaluation of Water Resources (APHRODITE) dataset

collected more rainfall observations across South Asia (Rana et al., 2015), which have been proved

could better estimate spatial precipitation (Andermann et al., 2011). Nonetheless, the lack and

uneven distribution of rainfall stations at high altitudes in the Tibetan Plateau and Himalayas may

introduce uncertainty and affect the accuracy of APHRODITE estimates (Rana et al., 2015;

Chaudhary et al., 2017).

Numerous rainfall observations can be obtained from public databases, although their short record

and static character limit their direct application in precipitation analysis (Donat et al., 2013).

However, these data could be useful for bias correction of gauge-based gridded products by

providing additional observations from the denser network of rainfall stations. On the other hand,

ranging from simple linear scaling to more sophisticated nonlinear approaches, several methods

have been developed to adjust global climate model (GCM) data (Teutschbein and Seibert, 2012).

Similarly, these bias correction methods could be applied to correct gridded rainfall products in

sparsely-gauged mountainous basins (He et al., 2017). It is important to study whether extreme

precipitation analysis could be improved by bias correction of gridded precipitation data and how

different methods would influence extreme precipitation indices.

This study evaluated different bias correction approaches for APHRODITE estimates in the YBRB

and assessed their effects on extreme precipitation analysis. We first corrected APHRODITE

estimates by both linear and nonlinear methods. Next, we calculated extreme precipitation indices

using original and different corrected APHRODITE estimates, and the effects of bias correction on

extreme precipitation analysis were further investigated by cross-validation. The results would support reference for the application of gridded precipitation data and bias-corrected methods in extreme precipitation analysis.

2   Material and methods

2.1   Study area

The YBRB can be divided into three physiographic zones: (1) the Tibetan plateau (TP), covering 44.4% of the basin, with elevations above 3500 m; (2) the Himalayan belt (HB), accounting for 28.6% of the basin, with elevations ranging from 100 m to 3500 m; and (3) the floodplains (FP), covering 27.0% of the basin, with elevations up to 100 m (Immerzeel, 2008).

The moisture in the YBRB is mainly from the Indian Ocean. The YBRB exhibits a broad range of precipitation from the semi-arid upstream areas to the HB characterized by abundant orographic rainfall as well as the vast humid FP. In the upstream areas, precipitation is concentrated during JJAS, and rainfall intensity is mostly low due to long-distance moisture transport (Guan et al., 1984). The irregular topographic variations in the Himalayas profoundly affect the spatial distribution of precipitation by altering monsoonal flow, producing intense orographic rainfall along the Himalayan foothills (Khandu et al., 2017). The downstream areas also receive high rainfall from monsoon flow during JJAS, accounting for 60%−70% of the annual rainfall (Gain et al., 2011).

2.2   Data sources

2.2.1   Observational data

In the upper YBRB, rainfall data across China recorded at 31 meteorological stations were collected

from the National Meteorological Information Center (NMIC, sourced from the China Meteorological Data Sharing Service System). In addition, data observed at 91 rainfall stations in the downstream area were obtained from the Global Historical Climatology Network (GHCN)−Daily dataset for bias correction. GHCN-Daily dataset comprises observations from four sources, which have been undergone extensive quality reviews, including the U.S. Collection, the International Collection, the Government Exchange Data, and the Global Summary of the Day. The locations of rainfall stations are shown in Fig. 1.

2.2.2 APHRODITE estimates

Numerous rainfall observations were incorporated into APHRODITE estimates, including (1) Global Telecommunication System (GTS)-based data, (2) data obtained from other projects or organizations, and (3) their own collection. The rainfall observations that had undergone quality control were gathered, and the ratios of rainfall observations to the world climatology were calculated and then interpolated for each month. The interpolated ratios were multiplied by the world climatology, and the first six components of the fast Fourier transform of the resulting values were used to obtain daily precipitation (Yatagai et al., 2012).

Daily rainfall data of APHRO_MA_025deg_V1101 (http://aphrodite.st.hirosaki-u.ac.jp/index.html) at 0.25° resolution in the Asian monsoon area end in 2007, while recently published APHRO_MA_025deg_V1101EX_R1 (http://aphrodite.st.hirosaki-u.ac.jp/index.html), using the same algorithm and spatial resolution, extend the time series over the period 2007−2015. Therefore, extreme precipitation could be analyzed during 1951−2015 by applying both datasets. To investigate the influence of topography on bias-corrected APHRODITE estimates, the grids were classified into

three topographic zones (the TP, HB, and FP; Fig. 2).

2.3 Methods

2.3.1 Bias correction methods

Two linear methods (linear scaling (LS) and local intensity scaling (LOCI)) and two non-linear

methods (power transformation (PT) and quantile−quantile mapping (QM)) were used for bias

correction in this study.

(1) LS

LS corrects monthly estimates in accordance with observations (Lenderink et al., 2007). It corrects

APHRODITE estimates using the ratio between mean monthly observation and corresponding

estimation:

$$P_{APH}^*(d) = P_{APH}(d) \cdot \left[\frac{\mu_m(P_{obs}(d))}{\mu_m(P_{APH}(d))} \right] \tag{1}$$

where $P_{APH}^*(d)$ and $P_{APH}(d)$ are the daily precipitation of corrected and original APHRODITE

estimate, respectively, and $P_{obs}(d)$ is the daily precipitation observed at the rainfall station in

corresponding grid of the APHRODITE estimate. $\mu_m(P_{obs}(d))$ and $\mu_m(P_{APH}(d))$ are the mean

monthly precipitation of observations and corresponding APHRODITE estimates in the mth month,

respectively.

(2) LOCI

LOCI makes a flexible adjustment to the wet-day frequency and intensity (Schmidli et al., 2006;

Teutschbein and Seibert, 2012). Firstly, an adjusted precipitation threshold ($P_{th,APH}$) is determined

so that the number of days exceeding this threshold for APHRODITE estimates matches that of

observed days with precipitation larger than 0 mm. Secondly, a linear scaling factor (s) for wet days

is computed:

$$s = \frac{\mu_m \left(P_{obs}(d) \big| P_{obs}(d) > 0 \text{ mm} \right)}{\mu_m \left(P_{APH}(d) \big| P_{APH}(d) > P_{th,APH} \right) - P_{th,APH}} \tag{2}$$

where $\mu_m \left(P_{obs}(d) \big| P_{obs}(d) > 0 \text{ mm} \right)$ is the mean monthly precipitation of observations with daily

precipitation larger than 0 mm, and $\mu_m \left(P_{APH}(d) \big| P_{APH}(d) > P_{th,APH} \right)$ is the mean monthly precipitation

of APHRODITE estimates with daily precipitation larger than $P_{th,APH}$. Finally, the precipitation data

are corrected, using:

$$P^*_{APH}(d) = \max \left(s \cdot \left(P_{APH}(d) - P_{th,APH} \right), 0 \right) \tag{3}$$

(3) PT

PT corrects both the mean and the coefficient of variation of precipitation (Leander and Buishand,

2007), changing precipitation by:

$$P^*_{APH}(d) = a \cdot \left(P_{APH}(d) \right)^b \tag{4}$$

where a and b are the parameters of the power transformation, which are obtained using a

distribution-free approach and estimated for each month within a 90-day window. Using a root-

finding algorithm, the value of b is firstly determined to ensure that the coefficient of variation of

the corrected estimates matches that of the observations. The parameter a is then calculated using

the mean observation and the corresponding mean of the transformed values.

(4) QM

By shifting occurrence distributions, QM corrects the distribution function of precipitation estimates

to match that of observations, which is commonly used in correcting systematic distributional biases

(Cannon et al., 2015). A Gamma distribution is usually assumed for precipitation events

(Teutschbein and Seibert, 2012):

$$f_\gamma\left(x|\alpha,\beta\right) = x^{\alpha-1} \cdot \frac{1}{\beta^\alpha \cdot \Gamma(\alpha)} \cdot e^{-\frac{x}{\beta}}; x \geq 0; \alpha, \beta > 0 \tag{5}$$

where α and β are the shape parameter and scale parameter, respectively.

The cumulative density function (CDF) of the APHRODITE estimates is adjusted to agree with that of the observation, and the daily precipitation for APHRODITE estimates is corrected depending on its quantile. It should be noted that for APHRODITE estimates, many days had low precipitation estimates instead of substantial dry conditions, which may distort the distribution of daily precipitation. Therefore, an adjusted precipitation threshold is also used to ensure the wet-day frequency of corrected APHRODITE estimates match the observed frequency:

$$P_{APH}^*\left(d\right) = \begin{cases} 0, & \text{if} \quad P_{APH}\left(d\right) < P_{th,APH} \\ F_\gamma^{-1}\left(F_\gamma\left(P_{APH}\left(d\right)|\alpha_{APH,m},\beta_{APH,m}\right)|\alpha_{obs,m},\beta_{obs,m}\right), & \text{otherwise} \end{cases}$$

(6)

F_γ and F_γ^{-1} are the Gamma CDF and its inverse, respectively. $\alpha_{APH,m}$ and $\beta_{APH,m}$ are the shape parameter and scale parameter of original APHRODITE estimates in the mth month, respectively, and $\alpha_{obs,m}$ and $\beta_{obs,m}$ are those of observations in the mth month, respectively.

This study corrected the grids of the APHRODITE estimates that contained time series of observations, and the parameters of bias correction were determined using corresponding available rainfall observations. After that, the APHRODITE estimates during 1951−2015 in these grids were corrected by 4 bias correction methods, respectively. Hereafter, APHRODITE estimates corrected by LS, LOCI, PT, and QM are referred as LS-APHRODITE, LOCI-APHRODITE, PT-APHRODITE, and QM-APHRODITE estimates, respectively.

2.3.2 Indices of extreme precipitation

To characterize extreme precipitation during JJAS, six indices recommended by the Expert Team

on Climate Change Detection and Indices (ETCCDI), including consecutive wet days (CWD), number of heavy precipitation days (R10mm), number of very heavy precipitation days (R20mm), maximum 1-day precipitation amount (Rx1d), maximum 5-day precipitation amount (Rx5d), and simple daily intensity index (SDII), were applied in this study. Detailed descriptions of these indices are shown in Table 1. The indices fall roughly into three categories: (1) duration indices, which represent the length of the wet spell; (2) threshold indices, which count the days on which a fixed precipitation threshold is exceeded; (3) absolute indices, which describe the maximum 1-day or 5-day precipitation amount (Sillmann et al., 2013).

Extreme precipitation indices for corrected APHRODITE estimates in the grids distributed with rainfall stations were calculated. To obtain extreme precipitation indices in other grids, inverse distance weighted (IDW) interpolation for extreme precipitation indices were performed. This allowed us to calculate mean values for each of the three topographic zones.

2.3.3 Validation on bias correction

Cross-validation was used to evaluate the performance of 4 bias correction methods. At each rainfall station, the observations were divided into two groups. Two third of the rainfall records were applied to calculate the parameters of bias correction, and then APHRODITE estimates were corrected. Making use of the remaining rainfall observations, the mean error (ME) of the extreme precipitation indices for corrected APHRODITE estimates were calculated to evaluate the performance of different bias correction methods.

3   Results

3.1 Extreme precipitation indices calculated from original and corrected APHRODITE estimates

3.1.1 Extreme precipitation indices in the three physiographic zones

Extreme precipitation indices calculated from original and four corrected APHRODITE estimates in the three different physiographic zones are shown in Fig. 3. The CWD estimated using original APHRODITE and LS-APHRODITE estimates were similar. Meanwhile, those derived from LOCI-, PT-, and QM-APHRODITE estimates were much less.

Mean R10mm during JJAS obtained by original APHRODITE estimates in the TP, HB, and FP were 6.7, 31.0, and 47.7 days, respectively. These were similar to those estimated by corrected APHRODITE estimates. However, the differences in R20mm were much pronounced. Mean R20mm in HB and FP for bias-corrected APHRODITE datasets were close to 19.0 and 26.5 days, respectively, which were approximately 4–5 days higher than those derived from original APHRODITE estimates.

Compared with original APHRODITE estimates, the Rx1d and Rx5d increased greatly after bias correction. In the HB, the mean Rx1d obtained from original APHRODITE estimates was 49.5 mm, while those for LS-, LOCI-, PT-, and QM-APHRODITE estimates were 72.4, 90.1, 109.0, and 103.8 mm, respectively. In addition, the ranges of Rx1d and Rx5d also increased considerably.

The differences in SDII between original and corrected APHRODITE estimates were also marked. For example, mean SDII in the FP calculated from original APHRODITE estimates was 13.4 mm. After correction, mean SDII for LOCI- and QM-APHRODITE estimates increased to 23.4 and 25.1 mm, respectively. These values were much greater than those derived from LS- and PT-APHRODITE datasets (15.7 and 17.7 mm).

3.1.2 Relative changes in extreme precipitation indices

The relative changes in extreme precipitation indices during JJAS based on original and corrected APHRODITE estimates are shown in Fig. 4. The CWD for LOCI-, PT-, and QM-APHRODITE estimates were all lower than original APHRODITE estimates, yielding relative change rates from −66% to −27%. Bias correction decreased the number of rainy days except LS. The variations in R10mm and R20mm illustrated that corrected APHRODITE estimates identified much more extreme precipitation events in the TP. The changes in indices varied considerably for different correction methods, with the change rates of R20mm in the TP for LS-, LOCI-, PT-, and QM-APHRODITE estimates being 30.4%, 169.2%, 297.1%, and 317.4%, respectively. For Rx1d, Rx5d, and SDII, the increases in the HB were much pronounced than those in the FP and TP. Except for LS-APHRODITE estimates, the increases in Rx1d and Rx5d in the HB were all above 70% for corrected APHRODITE estimates.

3.2 Influence of bias correction on extreme precipitation indices

3.2.1 Evaluation of extreme precipitation indices

The *ME* of extreme precipitation indices during JJAS for validation are shown in Fig. 5. For original APHRODITE estimates, the *ME* of CWD in the TP, HB, and FP were 8.3, 16.4, and 21.8 days, respectively. There were a lot of days with low precipitation estimations instead of substantial dry conditions, leading to the overestimation on CWD. Likewise, this propagated to LS-APHRODITE estimates with similar *ME* of CWD, because there was no change made to the wet-day frequency. The *ME* of CWD in the TP, HB, and FP for LOCI-APHRODITE estimates were 3.1, 1.2, and 1.4

days, respectively, and those for QM-APHRODITE estimates were 2.5, 0.8, and 0.9 days, respectively. For both LOCI- and QM-APHRODITE estimates, the days with low precipitation estimations instead of substantial dry conditions were redefined as dry days using precipitation threshold, resulting in much less *ME* and more reliable CWD. Finally, although PT did not directly correct wet-day frequency, the CWD for PT-APHRODITE estimates were lower than those for original APHRODITE estimates because tiny precipitation were corrected.

Original APHRODITE tended to underestimate heavy and very heavy precipitation days. Bias correction reduced error on R10mm and R20mm except LS, and the absolute value of mean *ME* for LOCI-, PT-, and QM-APHRODITE estimates were mostly less than 1.0 days. LOCI, PT, and QM are able to effectively correct heavy and very heavy precipitation days.

For original APHRODITE estimates, the *ME* of Rx1d were −11.3, −89.1 and −50.5 mm in the TP, HB, and FP, respectively, and those of Rx5d reached −18.0, −167.4 and −76.8 mm, respectively. Original APHRODITE estimates greatly underestimated Rx1d and Rx5d. For corrected APHRODITE estimates, QM performed best on Rx1d, and the *ME* for QM-APHRODITE estimates were −0.1, −1.9 and −5.4 mm, respectively. LS and LOCI used consistent ratio in linear transformation, resulting in underestimation on Rx1d. In addition, LOCI outperformed other methods on Rx5d, and the overestimation in the HB and FP for PT- and QM-APHRODITE estimates were greater.

The *ME* of SDII for original APHRODITE estimates in the TP, HB, and FP were −2.4, −13.9 and −11.0 mm, respectively. Firstly, heavy and very heavy precipitation in the HB and TP were not fully captured by original APHRODITE estimates. Secondly, original APHRODITE estimates overestimated wet days, which distorted the estimation of precipitation intensity. Smaller error were

3.2.2   Spatial distribution of extreme precipitation

Rainstorms over the lower YBRB usually have the duration of 2−3 days (Dhar and Nandargi, 2000), and large multi-day precipitation events are crucial to the floods in the basin. Hence, the spatial distribution of Rx5d during JJAS based on original APHRODITE estimates were compared with corrected APHRODITE estimates in Fig. 6. For original APHRODITE estimates, the area with Rx5d higher than 300 mm only accounted for 2.0% of the basin, while the proportions for LS-, LOCI-, PT-, and QM-APHRODITE estimates were 10.9%, 18.7%, 21.7%, and 21.3%, respectively. The most profound difference between original and corrected APHRODITE estimates occurred over the windward slopes of the Himalayas before the river flows into the Brahmaputra valley. The Rx5d calculated from original APHRODITE estimates were lower than 300 mm, while much higher Rx5d were obtained after bias correction, yielding maxima of 946.6, 1030.3, 1105.1, and 1396.6 mm for LS-, LOCI-, PT-, and QM-APHRODITE estimates, respectively. The eastern Himalayas, acting as orographic barriers, push the southwest moist air upwards, leading to heavier extreme precipitation over the windward slopes (Singh et al., 2004; Bookhagen and Burbank, 2010; Dimri et al., 2016). However, original APHRODITE estimates tended to substantially underestimate these extreme precipitation. Besides aforementioned region, higher Rx5d along the Himalayan front were also found after bias correction. In this case, extreme precipitation calculated from nonlinear approaches were heavier than those derived from linear methods. In general, bias correction are able to consider topographic effects on the spatial distribution of extreme precipitation more comprehensively.

4 Discussion

Using two linear and two nonlinear bias methods, we corrected APHRODITE estimates during JJAS in the YBRB to investigate the effects of different approaches on extreme precipitation analysis. Extreme precipitation indices were strongly dependent on the bias correction approach applied.

A primary problem when using gauge-based gridded data sets for extreme precipitation analysis is the fundamental mismatch between point-based observations and gridded estimates (Alexander, 2016). In addition, the spatial coverage of rainfall stations is another major source of uncertainty, particularly where spatial distributions of precipitation are complex (Donat et al., 2013). There are currently several approaches for bias correction, ranging from simple linear scaling to more sophisticated nonlinear methods (Teutschbein and Seibert, 2012). Although mean precipitation corrected by all bias-corrected approaches were similar, their standard deviations and consequent extreme precipitation indices varied considerably. In the case of linear correction, both mean and standard deviation are multiplied by same factor (Leander and Buishand, 2007), resulting in dubious variations of precipitation. Nonlinear correction adjust mean and also coefficient of variation (Teutschbein and Seibert, 2012), yielding more reliable results. In addition, the typical biases of rainfall products are related to their identification of too many wet days with low-intensity precipitation. Among the four bias-corrected approaches applied herein, LS and PT make no change on the number of rainy days, while LOCI and QM use threshold exceedance to match the wet-day frequency to the observations.

In international river basins, rainfall data are usually not publicly available, and extreme precipitation analysis may suffer from data restrictions (Nishat and Rahman, 2009; Luo et al., 2019).

Several great international rivers in south Asia, including the Indus, Ganges, and Yarlung

Tsangpo−Brahmaputra, originate from or flow through the Himalayas. Topographic variations of

the Himalayas profoundly influence the spatial distribution of precipitation by altering monsoonal

flow, resulting in considerable orographic rainfall on the windward slopes (Khandu et al., 2017).

Rainfall estimates of different products varied markedly along the Himalayan front and obtained

similar results toward the adjacent low-relief domains (Andermann et al., 2011). The GHCN-Daily

data can be applied to correct gauge-based gridded data sets in this region, ensuring these products

capture the spatial distribution and variation of extreme precipitation. However, numerous GHCN-

Daily records in Asia do not contain data from recent years, and the short or incomplete rainfall

records limit their direct applications (Donat et al., 2013). Hence, it would be preferable to apply

nonpublic datasets in data-sparse regions.

5   Conclusions

Despite increasing use of gridded rainfall products in sparsely gauged river basins, their application

in extreme precipitation analysis is challenging due to considerable biases. This study made use of

four methods to correct APHRODITE estimates in the YBRB. Their influences on extreme

precipitation indices were compared and assessed. The following conclusions were drawn.

(1) Original APHRODITE estimates tended to underestimate heavy and very heavy precipitation in

the YBRB, and there were a lot of days with low precipitation estimations instead of substantial dry

conditions. Bias correction greatly improved the performance of extreme precipitation analysis. The

extreme precipitation indices calculated from different corrected APHRODITE estimates varied

substantially, and LOCI- and QM-APHRODITE estimates were able to obtain more reliable extreme

precipitation indices.

(2) Insufficient gauge observations in the Himalayas caused high uncertainty in the heavy precipitation estimates for original APHRODITE estimates. After bias correction using observations from a denser network of gauges, the heterogeneous orographic effects on extreme precipitation were captured more accurately.

Data availability. The co-authors used publicly available data from the Asian Precipitation Highly Resolved Observational Data Integration Towards Evaluation of Water Resources and the National Centers for Environmental Information. In addition, rainfall observations in China were obtained from the National Meteorological Information Center.

Author contributions. XL and YL conceived the study, XL and XF carried out bias correction and extreme precipitation analysis, XL drafted the paper, and all co-authors jointly worked on enriching and developing the draft.

Competing interests. The authors declare that they have no conflict of interest.

References

Alexander, L. V.: Global observed long-term changes in temperature and precipitation extremes: A review of progress and limitations in IPCC assessments and beyond, Weather & Climate Extremes, 11, 4–16, https://doi.org/10.1016/j.wace.2015.10.007, 2016.

Andermann, C., Bonnet, S., and Gloaguen, R.: Evaluation of precipitation data sets along the Himalayan front, Geochemistry, Geophysics, Geosystems, 12, Q07023, https://doi.org/10.1029/2011gc003513, 2011.

Bookhagen, B., Burbank, and D. W.: Toward a complete Himalayan hydrological budget: Spatiotemporal distribution of snowmelt and rainfall and their impact on river discharge, Journal of Geophysical Research, 115, F03019, https://doi.org/doi:10.1029/2009JF001426, 2010.

Cannon A. J., Sobie S. R., Murdock T. Q.: Bias correction of GCM precipitation by quantile mapping: How well do methods preserve changes in quantiles and extremes? Journal of Climate, 28, 6938–6959, https://doi.org/10.1175/JCLI-D-14-00754.1, 2015.

Chaudhary S., Dhanya C. T., and Vinnarasi R.: Dry and wet spell variability during monsoon in gauge-based gridded daily precipitation datasets over India, Journal of Hydrology, 546, 204–218, https://doi.org/10.1016/j.jhydrol.2017.01.023, 2017.

Dhar, O. N. and Nandargi, S.: A study of floods in the Brahmaputra Basin in India, International Journal of Climatology, 20, 771–781, 2000.

Dimri, A. P., Thayyen, R. J., Kibler, K., Stanton, A., Jain, S. K., Tullos, D., and Singh, V. P.: A review of atmospheric and land surface processes with emphasis on flood generation in the Southern Himalayan rivers, Science of the Total Environment, 556, 98 – 115, http://dx.doi.org/10.1016/j.scitotenv.2016.02.206, 2016.

Donat, M.G., Alexander, L.V., Yang, H., Durre, I., Vose, R., and Caesar, J.: Global land-based

datasets for monitoring climatic extremes, Bulletin of the American Meteorological Society, 94, 997–1006, http://dx.doi.org/10.1175/BAMS-D-12-00109.1, 2013.

Easterling, D. R.: Climate extremes: observations, modeling, and impacts, Science, 289, 2068–2074, https://doi.org/doi:10.1126/science.289.5487.2068, 2000.

Gain, A. K., Immerzeel, W. W., Sperna Weiland, F. C., and Bierkens, M. F. P.: Impact of climate change on the stream flow of the lower Brahmaputra: trends in high and low flows based on discharge-weighted ensemble modelling, Hydrology and Earth System Sciences, 15, 1537–1545, https://doi.org/10.5194/hess-15-1537-2011, 2011.

Guan, Z. H., Chen, C. Y., Ou, Y. X., Fan, Y. Q., Zhang, Y. S., Chen, Z. M., Bao, S. H., Zu, Y. T., He, X. W., and Zhang, M. T. (Eds.): Rivers and Lakes in Tibet, Science Press, Beijing, China, pp. 35–39, 1984.

He, Z., Hu, H., Tian F., Ni G., and Hu Q.: Correcting the TRMM rainfall product for hydrological modelling in sparsely-gauged mountainous basins, Hydrological Sciences Journal, 62, 306–318, https://doi.org/10.1080/02626667.2016.1222532, 2017.

Immerzeel, W.: Historical trends and future predictions of climate variability in the Brahmaputra basin, International Journal of Climatology, 28, 243−254, https://doi.org/10.1002/joc.1528, 2008.

Immerzeel, W. W., van Beek, L. P. H., and Bierkens, M. F. P.: Climate change will affect the Asian water towers, Science, 328, 1382−1385, https://doi.org/10.1126/science.1183188, 2010.

Janes, T., Mcgrath, F., Macadam, I., and Jones, R.: High-resolution climate projections for south Asia to inform climate impacts and adaptation studies in the Ganges-Brahmaputra-Meghna and Mahanadi deltas, Science of The Total Environment, 650, 1499 – 1520, https://doi.org/10.1016/j.scitotenv.2018.08.376, 2019.

Kamal-Heikman, S., Derry, L. A., Stedinger, J. R., and Duncan, C. C.: A simple predictive tool for lower Brahmaputra River Basin monsoon flooding, Earth Interactions, 11, 1 – 11, https://doi.org/10.1175/EI226.1, 2007.

Khandu, Awange, J. L., Kuhn, M., Anyah, R., and Forootan, E.: Changes and variability of precipitation and temperature in the Ganges-Brahmaputra-Meghna River Basin based on global high-resolution reanalyses, International Journal of Climatology, 37, 2141−2159, https://doi.org/10.1002/joc.4842, 2017.

Lakshmi, V., Fayne, J., and Bolten, J.: A comparative study of available water in the major river basins of the world, Journal of Hydrology, 567, 510 – 532, https://doi.org/10.1016/j.jhydrol.2018.10.038, 2018.

Leander, R. and Buishand, T. A.: Resampling of regional climate model output for the simulation of extreme river flows, Journal of Hydrology, 332, 487 – 496, https://doi.org/10.1016/j.jhydrol.2006.08.006, 2007.

Lenderink, G., Buishand, A., and van Deursen, W.: Estimates of future discharges of the river Rhine using two scenario methodologies: direct versus delta approach, Hydrology and Earth System Sciences, 11, 1145–1159, https://doi.org/10.5194/hess-11-1145-2007, 2007.

Liu, Z., Wang, R., and Yao, Z.: Climate change and its impact on water availability of large international rivers over the mainland Southeast Asia, Hydrological Processes, 32, 3966−3977, https://doi.org/10.1002/hyp.13304, 2018.

Luo, X., Wu, W., He, D., Li, Y., and Ji, X.: Hydrological simulation using TRMM and CHIRPS precipitation estimates in the lower Lancang-Mekong River Basin, Chinese Geographical Science, 29, 13–25, https://doi.org/10.1007/s11769-019-1014-6, 2019.

Malik, N., Bookhagen, B., and Mucha, P. J.: Spatiotemporal patterns and trends of Indian monsoonal rainfall extremes, Geophysical Research Letters, 43, 1710, https://doi.org/doi:10.1002/2016GL067841, 2016.

Nishat, B. and Rahman, S. M. M.: Water resources modeling of the Ganges-Brahmaputra-Meghna River Basins using satellite remote sensing data, Journal of the American Water Resources Association, 45, 1313−1327, https://doi.org/10.1111∕j.1752-1688.2009.00374.x, 2009.

Pervez, M. S. and Henebry, G. M.: Spatial and seasonal responses of precipitation in the Ganges and Brahmaputra river basins to ENSO and Indian Ocean dipole modes: implications for flooding and drought, Nat. Hazards Earth Syst. Sci., 15, 147–162, https://doi.org/10.5194/nhess-15-147-2015, 2015.

Prakash, S., Mitra, A. K., Momin, I. M., Rajagopal, E. N., Basu, S., Collins, M., Turner, A. G., Rao, K. A., and Ashok, K.: Seasonal intercomparison of observational rainfall datasets over India during the southwest monsoon season, International Journal of Climatology, 35, 2326−2338, https://doi.org/10.1002/joc.4129, 2015.

Prakash, S., Seshadri, A., Srinivasan, J., and Pai, D. S.: A new parameter to assess impact of rain gauge density on uncertainty in the estimate of monthly rainfall over India, Journal of Hydrometeorology, 20, 821–832, https://doi.org/10.1175/JHM-D-18-0161.1, 2019.

Rana, S., McGregor, J., and Renwick, J.: Precipitation seasonality over the Indian subcontinent: an evaluation of gauge, reanalyses, and satellite retrievals, Journal of Hydrometeorology, 16, 631−651, https://doi.org/10.1175/jhm-d-14-0106.1, 2015.

Ray, P. A., Yang, Y. E., Wi, S., Khalil, A., Chatikavanij, V., and Brown, C.: Room for improvement: Hydroclimatic challenges to poverty-reducing development of the Brahmaputra River basin,

Environmental Science & Policy, 54, 64−80, https://doi.org/10.1016/j.envsci.2015.06.015, 2015.

Schmidli, J., Frei, C., and Vidale, P. L.: Downscaling from GCM precipitation: a benchmark for dynamical and statistical downscaling methods, International Journal of Climatology, 26, 679–689, https://doi.org/10.1002/joc.1287, 2006.

Sillmann, J., Kharin, V. V., Zhang, X., Zwiers, F. W., and Bronaugh, D.: Climate extremes indices in the CMIP5 multimodel ensemble: Part 1. Model evaluation in the present climate, Journal of Geophysical Research: Atmospheres, 118, 1716 – 1733, https://doi.org/doi:10.1002/jgrd.50203, 2013.

Singh, S., Kumar, R., Bhardwaj, A., Sam, L., Shekhar, M., Singh, A., Kumar, R., and Gupta, A.: Changing climate and glacio-hydrology in Indian Himalayan Region: a review. Wiley Interdisciplinary Reviews: Climate Change, 7, 393−410. https://doi.org/10.1002/wcc.393, 2016.

Singh, V. P., Sharma, N., and Ojha, C. S. P. (Eds.): The Brahmaputra Basin water resources, Kluwer Academic Publishers, Dordrecht, Netherlands, pp. 17−34, 2004.

Teutschbein, C. and Seibert, J.: Bias correction of regional climate model simulations for hydrological climate-change impact studies: Review and evaluation of different methods, Journal of Hydrology, 456–457, 12–29, https://doi.org/10.1016/j.jhydrol.2012.05.052, 2012.

Wang, C., Ren, X., and Li, Y.: Analysis of extreme precipitation characteristics in low mountain areas based on three-dimensional copulas—taking Kuandian County as an example, Theoretical and Applied Climatology, 128, 169–179, https://doi.org/10.1007/s00704-015-1692-7, 2017.

Xu, R., Hu, H., Tian, F., Li, C., and Khan, M. Y. A.: Projected climate change impacts on future streamflow of the Yarlung Tsangpo-Brahmaputra River, Global and Planetary Change, 175, 144–159, https://doi.org/10.1016/j.gloplacha.2019.01.012, 2019.

Yatagai, A., Kamiguchi, K., Arakawa, O., Hamada, A., Yasutomi, N., and Kitoh, A.: APHRODITE: Constructing a long-term daily gridded precipitation dataset for Asia based on a dense network of rain gauges, Bulletin of the American Meteorological Society, 93, 1401−1415, https://doi.org/10.1175/bams-d-11-00122.1, 2012.

Yucel, I. and Onen, A.: Evaluating a mesoscale atmosphere model and a satellite-based algorithm in estimating extreme rainfall events in northwestern Turkey, Nat. Hazards Earth Syst. Sci., 14, 611−624, https://doi.org/10.5194/nhess-14-611-2014, 2014.

Zhang Y., Zheng H., Herron N., Liu X., Wang Z., Chiew, F. H. S., and Parajka, J.: A framework estimating cumulative impact of damming on downstream water availability, Journal of Hydrology, 575, 612–627, https://doi.org/10.1016/j.jhydrol.2019.05.061, 2019.

Table 1. Detailed description of extreme precipitation indices.

Table 1. Detailed description of extreme precipitation indices.

Index	Descriptive name	Definition	Unit
CWD	Consecutive wet days	Maximum number of consecutive days with precipitation ≥ 1 mm	days
R10mm	Number of heavy precipitation days	Count of days when precipitation ≥ 10 mm during June, July, August, and September (JJAS)	days
R20mm	Number of very heavy precipitation days	Count of days when precipitation ≥ 20 mm during JJAS	days
Rx1d	Maximum 1-day precipitation amount	Maximum 1-day precipitation	mm
Rx5d	Maximum 5-day precipitation amount	Maximum consecutive 5-day precipitation	mm
SDII	Simple daily intensity index	Total precipitation during JJAS divided by the number of wet days (when precipitation ≥ 1 mm)	mm/day

Figure 1. Locations of rainfall stations in the Yarlung Tsangpo-Brahmaputra River Basin (YBRB).

Figure 2. Location of Asian Precipitation Highly Resolved Observational Data Integration Towards Evaluation of Water Resources (APHRODITE) grids over the Tibetan plateau (TP), Himalayan belt (HB), and floodplains (FP).

Figure 3. Box-whisker plot for (a) consecutive wet days (CWD), (b) number of heavy precipitation days (R10mm), (c) number of very heavy precipitation days (R20mm), (d) maximum 1-day precipitation amount (Rx1d), (e) maximum 5-day precipitation amount (Rx5d), and (f) simple daily intensity index (SDII) during June, July, August, and September (JJAS) in the three different physiographic zones (the TP, HB, and FP) of the YBRB derived from original and corrected APHRODITE estimates.

Figure 4. Relative change rate of (a) CWD, (b) R10mm, (c) R20mm, (d) Rx1d, (e) Rx5d, and (f) SDII during JJAS for original and corrected APHRODITE estimates.

Figure 5. Mean error (*ME*) of extreme precipitation indices during JJAS for validation in the three different physiographic zones (TP, HB, and FP) of the YBRB.

Figure 6. Spatial distribution of mean Rx5d during JJAS in the YBRB based on (a) original APHRODITE estimates, as well as (b) linear scaling (LS)-APHRODITE estimates, (c) local intensity scaling (LOCI)-APHRODITE estimates, (d) power transformation (PT)-APHRODITE estimates, and (e) quantile−quantile mapping (QM)-APHRODITE estimates.
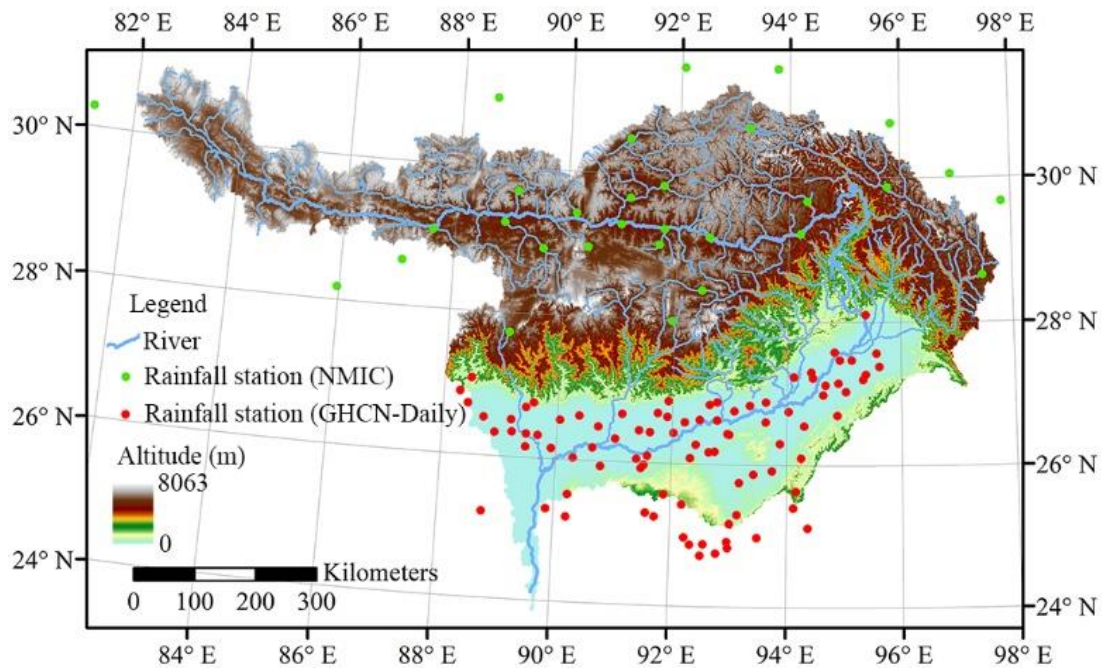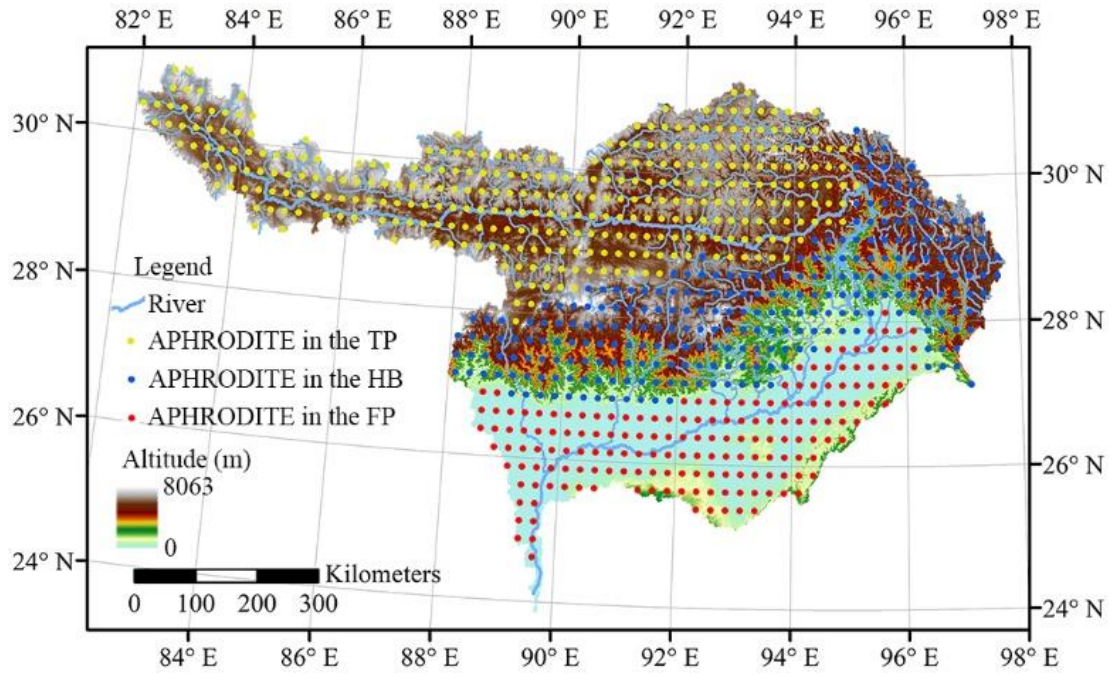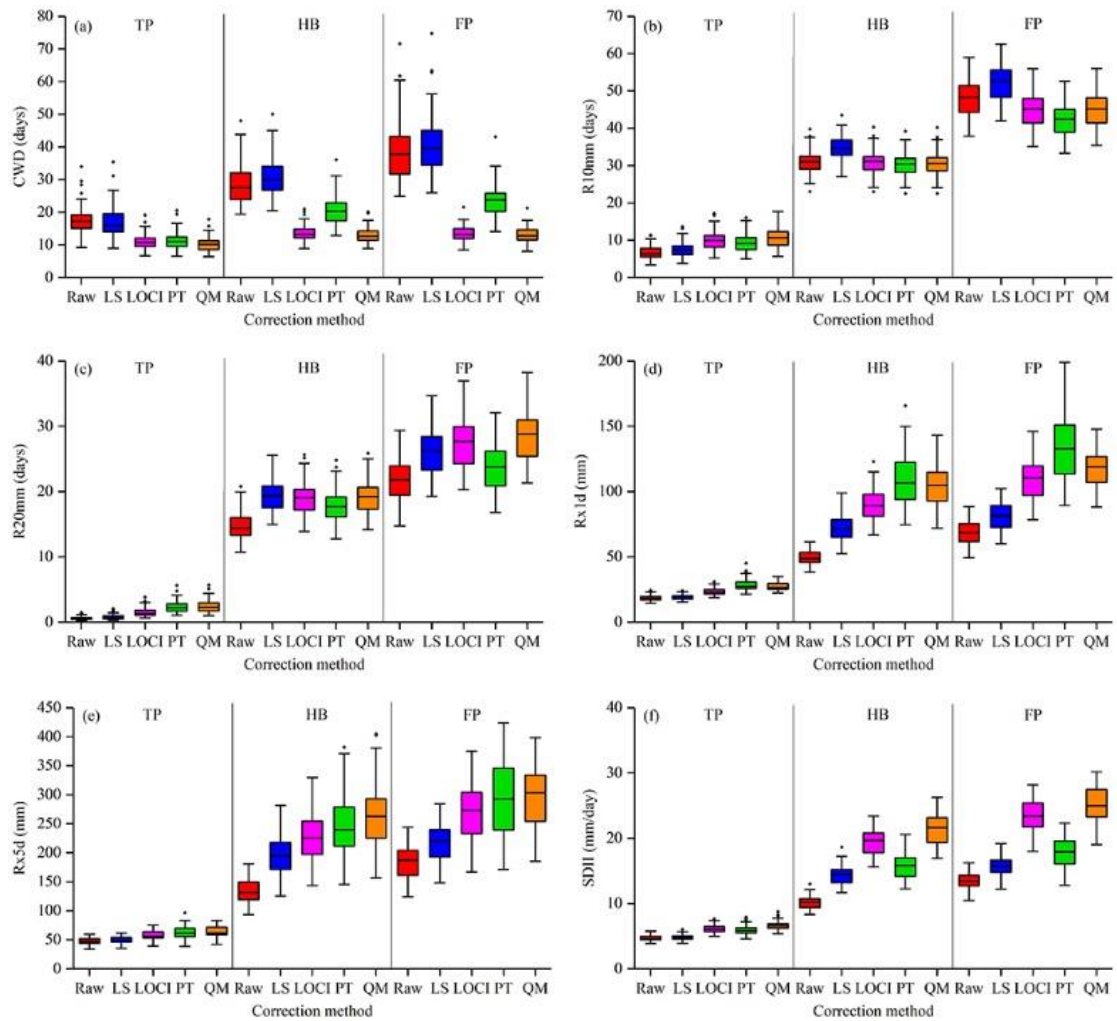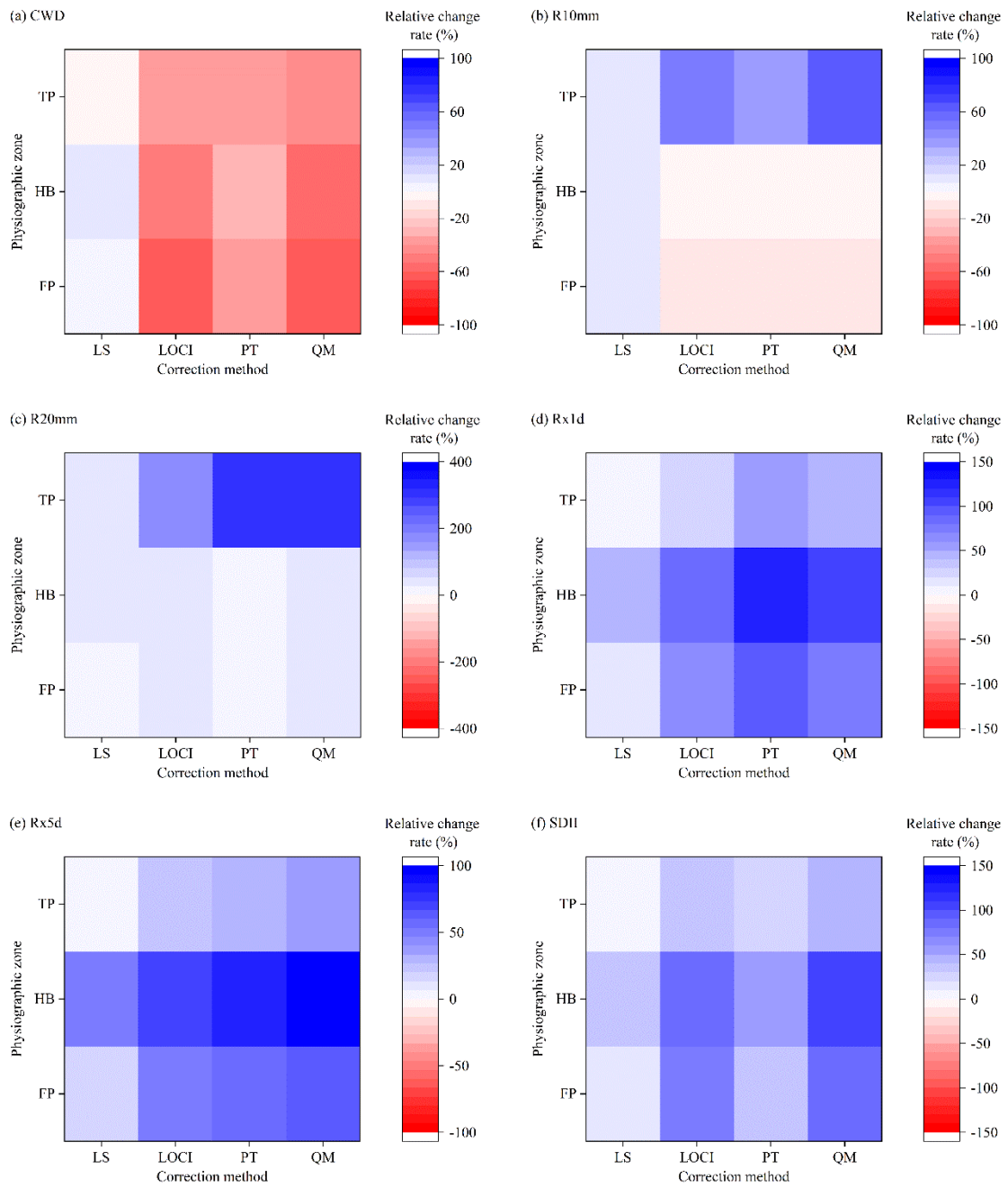
Figure 1. Locations of rainfall stations in the Yarlung Tsangpo-Brahmaputra River Basin (YBRB).

Figure 2. Location of Asian Precipitation Highly Resolved Observational Data Integration Towards Evaluation of Water Resources (APHRODITE) grids over the Tibetan plateau (TP), Himalayan belt (HB), and floodplains (FP).

Figure 3. Box-whisker plot for (a) consecutive wet days (CWD), (b) number of heavy precipitation days (R10mm), (c) number of very heavy precipitation days (R20mm), (d) maximum 1-day precipitation amount (Rx1d), (e) maximum 5-day precipitation amount (Rx5d), and (f) simple daily intensity index (SDII) during June, July, August, and September (JJAS) in the three different physiographic zones (the TP, HB, and FP) of the YBRB derived from original and corrected APHRODITE estimates.

Figure 4. Relative change rate of (a) CWD, (b) R10mm, (c) R20mm, (d) Rx1d, (e) Rx5d, and (f) SDII during JJAS for original and corrected APHRODITE estimates.
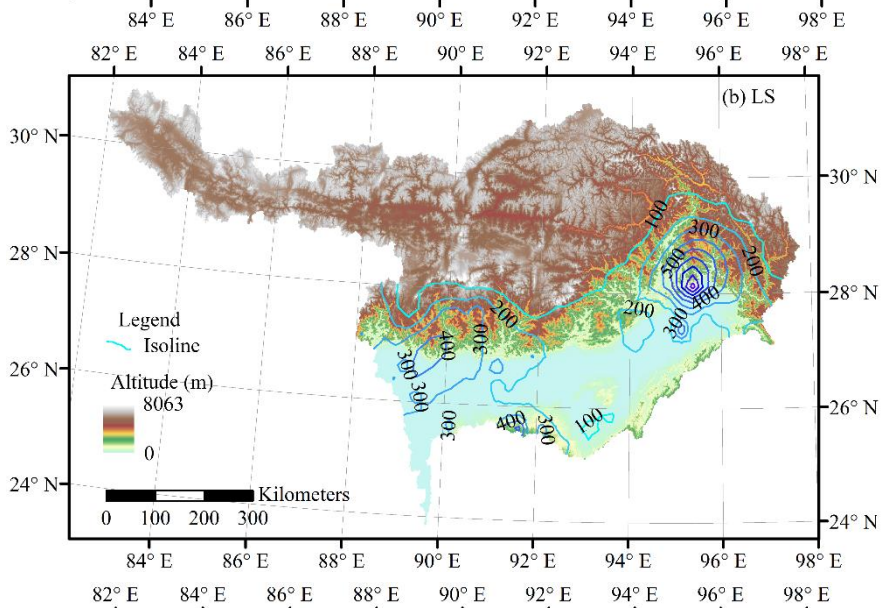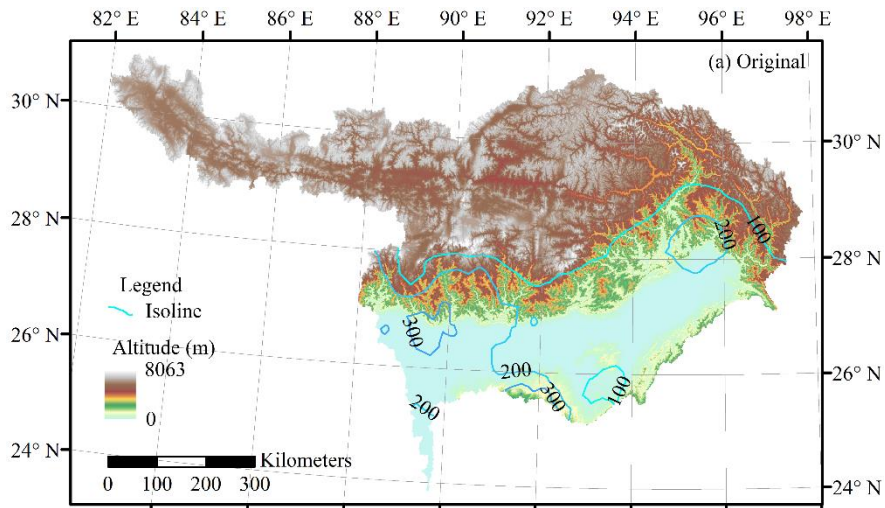
Figure 5. Mean error (*ME*) of extreme precipitation indices during JJAS for validation in the three different physiographic zones (TP, HB, and FP) of the YBRB.
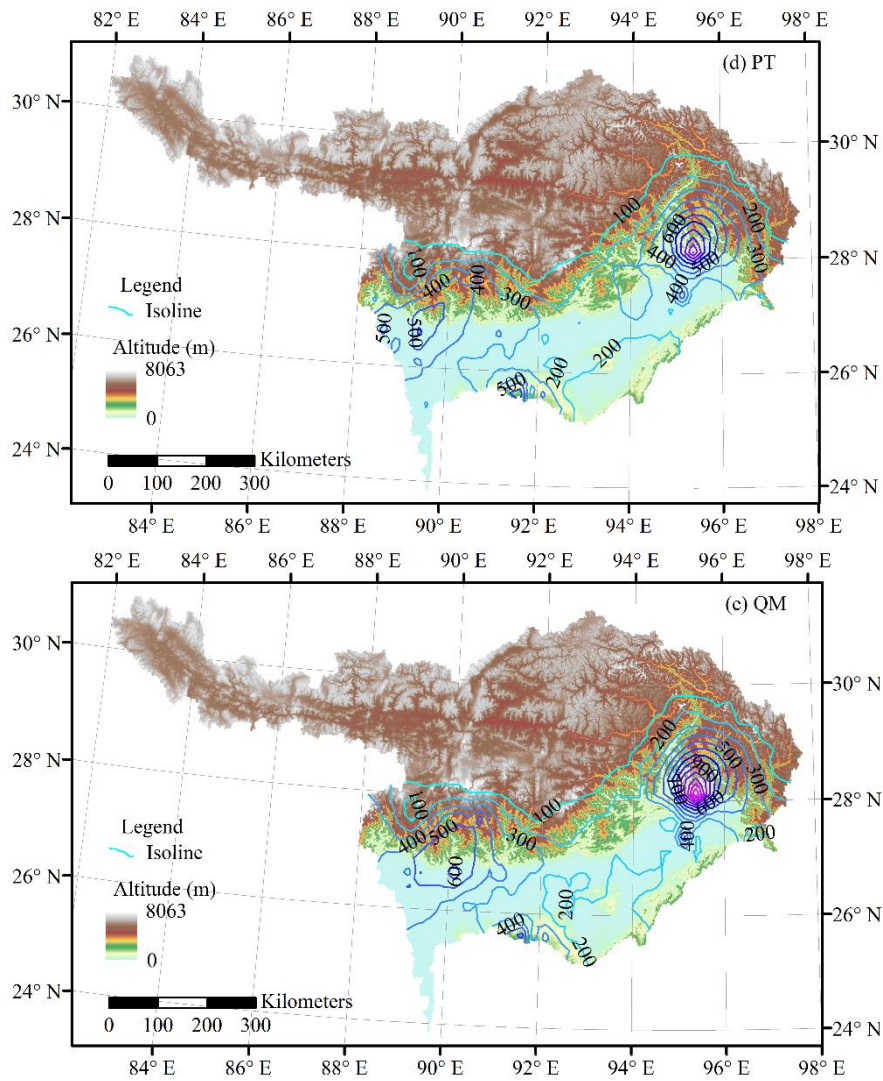
Figure 6. Spatial distribution of mean Rx5d during JJAS in the YBRB based on (a) original APHRODITE estimates, as well as (b) linear scaling (LS)-APHRODITE estimates, (c) local intensity scaling (LOCI)-APHRODITE estimates, (d) power transformation (PT)-APHRODITE estimates, and (e) quantile−quantile mapping (QM)-APHRODITE estimates.